

# Nonlocal growth processes and conformal invariance

Francisco C. Alcaraz<sup>1</sup> and Vladimir Rittenberg<sup>2</sup>

<sup>1</sup>*Instituto de Física de São Carlos, Universidade de São Paulo, Caixa Postal 369,  
13560-590, São Carlos, SP, Brazil*

<sup>2</sup>*Physikalisches Institut, Universität Bonn, Nussallee 12, 53115 Bonn, Germany*

June 12, 2018

## Abstract

Up to now the raise and peel model was the single known example of a one-dimensional stochastic process where one can observe conformal invariance. The model has one-parameter. Depending on its value one has a gapped phase, a critical point where one has conformal invariance and a gapless phase with changing values of the dynamical critical exponent  $z$ . In this model, adsorption is local but desorption is not. The raise and strip model presented here in which desorption is also nonlocal, has the same phase diagram. The critical exponents are different as are some physical properties of the model. Our study suggest the possible existence of a whole class of stochastic models in which one can observe conformal invariance.

## 1 Introduction

There is a long list of papers on one-dimensional interface growth models (see [1] and [2] for reviews). In most of them the stochastic processes are local. Two typical gapless phases are encountered: the Edwards-Wilkinson phase [3] where the dynamical critical exponent  $z = 2$  and the Kardar-Parisi-Zhang phase [4] where  $z = 3/2$ . If in a model one has an Edwards-Wilkinson phase by introducing an asymmetry one can get a Kardar-Parisi-Zhang phase. By introducing "friction" (some processes oppose growth) one gets a gapped phase (see the flip-flop model described below). The interplay of asymmetry and "friction" is nicely displayed in [5].

As far as we know the first example of a nonlocal growth model is the Derrida and Vannimenus' study of the interface in weakly disordered systems [6]. Much later another model with nonlocal rates appeared in the literature, the raise and peel model (RPM) [7]. This is a one-parameter (denoted by  $u$ ) dependent model which also displays three situations,

---

<sup>1</sup>alcaraz@if.sc.usp.br

<sup>2</sup>vladimir@th.physik.uni-bonn.de

analogously to local models. For small values of  $u$  one has a gapped phase, for  $u = 1$  one has a gapless phase with  $z = 1$  (not  $z = 2$ ) and for  $u > 1$  one has a gapless phase with varying values of  $z$  (this corresponds to the KPZ phase in local models). Dyck (special RSOS) paths describe the interface. Adsorption is local but desorption is nonlocal. The desorption processes look a bit artificial, they come from the algebraic background of the model at  $u = 1$ . What is special in this model is that for  $u = 1$  one can do analytic calculations and show that the model is conformal invariant. Moreover, the stationary state of the model has fascinating combinatorial properties [8, 9, 10]. Recently, another model (the peak adjusted raise and peel model (PARPM)) was introduced [11]. The adsorption and desorption processes are like in the RPM but the rates depend on the number of peaks in the Dyck paths. This makes the rates dependent on the size of the system. A new parameter  $p$  was introduced such that if  $p = 1$ , one recovers the RPM at  $u = 1$ . It was shown that conformal invariance is maintained in whole domain of  $p$ . In this paper we present a new model, the raise and strip model (RSM) which is again a one-parameter dependent model, with local adsorption and nonlocal desorption processes, the rules for the latter being much simpler. The configuration space is the same as in the RPM. Our aim was to see if the main ingredient to get conformal invariance is the existence of nonlocal processes of a special kind. We were aware that the price to pay is losing integrability and that one had to use Monte Carlo simulations on large lattices to get results. We have indeed observed that the RSM has a phase diagram similar to the one seen in the RPM. At the conformal invariant point, the critical exponents are different. Since other models having the same structure as the RSM can easily be defined, it is plausible to assume that there is a whole class of models with conformal invariance which should be studied.

The paper is organized as follows. In Section 2 we defined the observables for models defined on Dyck paths. These observables are used in the description of the properties of the models.

The flip-flop, the raise and peel and raise and strip models are defined in Section 3. The flip-flop model is the local version of the RSM, it was studied in order to see the effect of nonlocality introduced in the RSM.

The flip-flop model is presented in Section 4. One shows, using known results from combinatorics and Monte Carlo simulations that one has a critical point with a dynamic critical exponent  $z = 2$  which separates two gapped phases.

The raise and peel model is shortly reviewed in Section 5.

The main results of our research are given in Section 6 in which we present not only the properties of the stationary states of the RSM but also the time dependent phenomena. An interesting new phenomenon occurs if the parameter  $u$  is larger than  $u_c$ . The system stays gapless with varying values of  $z$  (like in the RPM) but unlike the RPM where in the stationary state, the average height increases logarithmically with the size of the system, in the RSM, the average height profile is a triangle with a height of the order of the system size.

For completeness, a variant of the flip-flop model in which the configuration space is changed, is presented in the Appendix.

Our conclusions can be found in Section 7

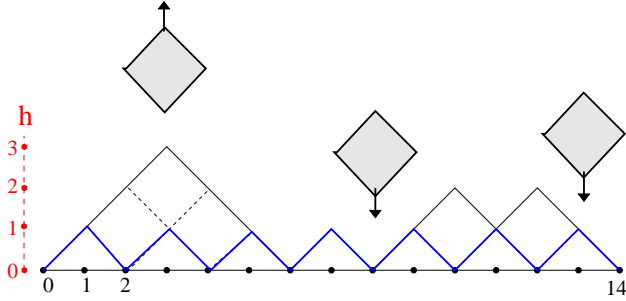


Figure 1: An example of a Dyck path for  $L = 14$ . There are four contact points, three clusters, four peaks and three valleys. The substrate profile is shown in blue.

## 2 Observables for models defined on Dyck paths

We consider an open one-dimensional system with  $L + 1$  sites ( $L$  even). A Dyck path is a special restricted solid-on-solid (RSOS) configuration defined as follows. We attach to each site  $i$  integer heights  $h_i$  which obey RSOS rules:

$$h_{i+1} - h_i = \pm 1, \quad (i = 0, 1, \dots, L - 1), \quad (2.1)$$

with the constraints:

$$h_0 = h_L = 0, \quad (2.2)$$

$$h_i \geq 0, \quad (i = 0, 1, \dots, L). \quad (2.3)$$

There are

$$Z(L) = L! / (L/2)! (L/2 + 1)! \quad (2.4)$$

configurations of this kind.

A Dyck path can be seen as an interface separating a film of tilted tiles deposited on a substrate, from a rarefied gas of tiles (see Fig. 1). The substrate corresponds to the special Dyck path defined as  $h_{2k} = 0$ ,  $h_{2k+1} = 1$  ( $k = 0, 1, \dots, L/2 - 1$ ).

If  $h_j = 0$  at the site  $j$ , one has a *contact point* (there are four contact points in Fig. 1). Between two consecutive contact points one has a *cluster* (there are three clusters in Fig. 1). The slope at the site  $i$  is  $s(i) = (h_{i+1} - h_{i-1})/2$ . If  $s_i = 0$  ( $h_i > h_{i-1}$ ) one has a *peak*. If  $s_i = 0$  ( $h_i < h_{i-1}$ ) one has a *valley* (there are four peaks and three valleys in Fig. 1).

It is useful to use the known mapping between an RSOS path and the configuration space of a one-dimensional hopping model with exclusion. To an upwards step  $h_i - h_{i-1} > 0$  one associates a particle, to an downwards step  $h_i - h_{i-1} < 0$  one associates a vacancy. The constraints (2.2)-(2.3) are translated into two conditions on the particles-vacancies configurations. The first constraint (2.2) implies that the number of particles is equal to the number of vacancies. The second constraint (2.3) is obviously nonlocal: the number of particles on the left side of any bond has to be larger or equal to the number of vacancies on the left side of the same bond. For example, the configuration  $XXOXOO$  is acceptable but not  $OOXOXX$  ( $X$  is a particle,  $O$  is a vacancy). The Dyck path shown in Fig. 1 corresponds to the configuration  $XXXOOOXOXXOXOO$ .

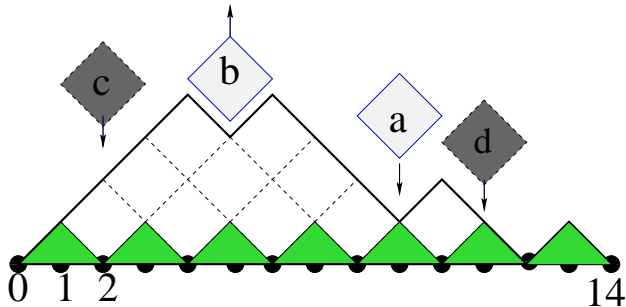


Figure 2: The flip-flop model. When a tile hits the interface, the following processes occur: The tiles  $c$  and  $d$  are reflected, tile  $b$  triggers a local desorption and the tile  $a$  which hits a valley, is adsorbed.

The raise and fall stochastic models to be described below give the probabilities of the various Dyck paths and one is interested in average values of observables.

One obvious observable is  $h(i, L, t)$  which is the average height at the site  $i$  for a system of size  $L$  and time  $t$ . The average density of contact points which is a function of the site  $i$ , the size  $L$  of the system and  $t$ , will be denoted by  $g(i, L, t)$ . The average density of clusters equal to the average number of clusters divided by  $L$ , will be denoted by  $K(L, t)$ . When one considers the stationary states of the models, the time dependence will be dropped in the notation. For example,  $g(i, L, t)$  will become  $g(i, L)$ . It turns out that the average density of peaks and valleys  $\tau(L, t)$ , equal to the average total number of peaks and valleys divided by  $L$ , plays an important role in studying the properties of the models.

### 3 Raise and fall models

We present three stochastic models defined in the configuration space of Dyck paths. In one of the models (the flip-flop model) the processes are local, in the other two (the raise and peel and raise and strip models), the adsorption processes are nonlocal. As we are going to see it is the nonlocality of the rates which is relevant in getting new physics.

The models depend on one parameter  $u$  which is the ratio of adsorption and desorption rates. One uses sequential updating. At each time step, with a probability  $1/(L - 1)$  a tile hits the Dyck path at a site  $i = 1, 2, \dots, L - 1$ . The effects of the hits are different in the three models.

The *flip-flop model* (FFM) is an extension of the freely jointed chain model of a random coil polymer [12]. In this model both the adsorption and desorption processes are local. The nonlocality comes only from the constraint (2.3) which defines the Dyck paths and, unlike the two other models, not from the rates. The model is defined by the following rules:

If a tile hits a valley ( $s_i = 0$  and  $h_i < h_{i-1}$ ), with a rate  $u$  it sticks to the site and the valley becomes a peak (see tile  $a$  in Fig. 2). If a tile hits a peak ( $s_i = 0$  and  $h_i > h_{i-1} > 0$ ), with a rate equal to one, the tile at the peak gets desorbed and the peak becomes a valley (see tile  $b$  in Fig. 2). If the tile hits a site  $i$  and  $s_i \neq 0$ , the tile is reflected with no changes in the profile (see tiles  $c$  and  $d$  in Fig. 2). In this model the rates are local. In the raise

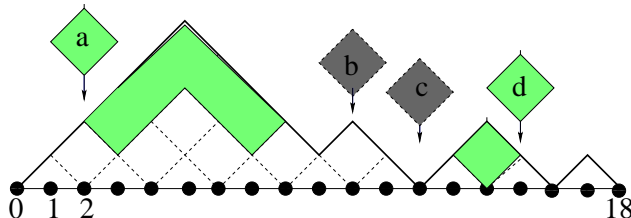


Figure 3: The raise and peel model. When tile  $a$  hits the interface it triggers a nonlocal desorption. The desorption can be local only if the tile hits the substrate (tile  $d$ ). If the tile hits a peak, it is reflected (tile  $b$ ). If a tile hits a valley, like in the flip-flop model, the tile is adsorbed (tile  $c$ ).

and strip model to be described below the desorption rates are nonlocal and it is interesting therefore to compare the models.

The *raise and peel model* (RPM) was intensively studied [7]. We present it here in order to clarify the effects of nonlocality on the physics of the models.

The main merit of the RPM is that for  $u = 1$ , it is integrable and conformal invariant. The essential features of the model are local adsorption and nonlocal desorption processes of a particular kind. The rules for the latter come from the algebraic structure (the Temperley-Lieb algebra) behind the model. These rules do not easily generalize for other configuration spaces where we expect to be able, based on algebraic considerations (using Hecke algebras), to define stochastic models which are also conformal invariant. An example is the case of restricted Motzkin paths [13]. The RPM is defined by the following rules:

Depending on the slope  $s_i = (h_{i+1} - h_{i-1})/2$  at the site  $i$ , the following processes can occur:

- 1)  $s_i = 0$  and  $h_i < h_{i-1}$  (tile  $c$  in Fig. 3). The tile hits a local minimum and with a rate  $u$  is adsorbed ( $h_i \rightarrow h_i + 2$ ).
- 2)  $s_i = 0$  and  $h_i > h_{i-1}$  (tile  $b$  in Fig 3). The tile hits a peak and is reflected.
- 3)  $s_i = 1$  (tile  $a$  in fig. 3). With a rate one the tile is reflected after triggering the desorption ( $h_j \rightarrow h_j - 2$ ) of a layer of  $b - 1$  tiles from the segment  $\{j = i + 1, \dots, i + b - 1\}$  where  $h_j > h_i = h_{i+b}$ .
- 4)  $s_i = -1$  (tile  $d$  in Fig. 3). With a rate one, the tile is reflected after triggering the desorption ( $h_j \rightarrow h_j - 2$ ) of a layer of  $b - 1$  tiles belonging to the segment  $\{j = i - b + 1, \dots, i - 1\}$  where  $h_j > h_i = h_{i-b}$ .

The *raise and strip model* (RSM) was conceived in order to keep the main features of the RPM (local adsorption and nonlocal desorption) using simpler rules and to see if one can recover conformal invariance. The price to pay is of course, lack of integrability and other magic properties of the RPM. Keeping in mind that in a Dyck path each valley is followed by a peak and that a peak is surrounded by two consecutive valleys, the RSM is defined by the following rules:

If a tile hits a valley ( $s_i = 0$  and  $h_i < h_{i-1}$ ), with a rate  $u$  it sticks to the site and the valley becomes a peak (see tile  $a$  of Fig. 4). If a tile hits a peak ( $s_i = 0$  and  $h_i > h_{i-1} > 0$ ), surrounded by two valleys at the sites  $k$  and  $l$  ( $k < i < l$ ), with a rate equal to one, a layer of tiles between the two consecutive valleys is desorbed (see tile  $b$  of Fig. 4). One has

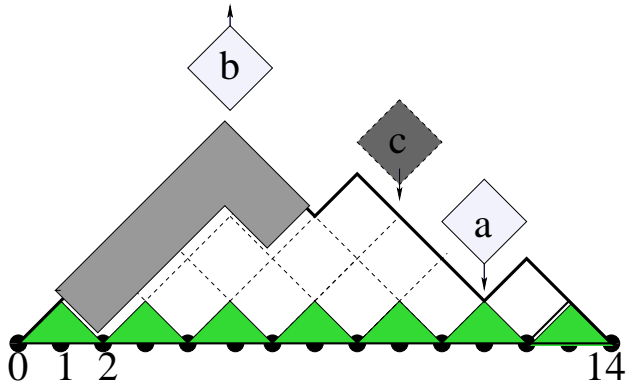


Figure 4: The raise and strip model. When a tile hits a peak it triggers a nonlocal desorption process (tile  $b$ ), the tile is reflected otherwise (tile  $c$ ) unless it hits a valley when it gets adsorbed (tile  $a$ ).

$h_j \rightarrow h_j - 2$  ( $j = k + 1, k + 2, \dots, l - 1$ ). If the tile hits a site  $i$  and  $s_i \neq 0$ , like in the FFM but unlike the RPM, the tile is reflected (see tile  $c$  of Fig. 4).

We notice that the adsorption process is common to all three models. The differences are in the desorption processes. They are similar in the RSM and RPM: in general a layer of tiles evaporates and not a single tile. This is why one expects to find in the RSM model a value of the parameter  $u$  for which one could see conformal invariance like in the RPM.

In the FFM and RSM the desorption takes place when a tile hits a peak and is reflected when the tile hits a site with no valleys or peaks. In the first model desorption is local but is nonlocal in the RSM. The number of active sites for desorption is equal to the number of active sites for adsorption. In the RPM this is not anymore the case, the number of active sites for desorption being the sites with  $s_i \neq 0$ .

The differences between the three models mentioned above will determine major differences in their physical properties which are going to be discussed in the next sections.

In order to study the continuous time evolution in the three models described above, one uses the master equation which can be interpreted as an imaginary time Schroedinger equation. If the system is composed by the states  $a = 1, 2, \dots, Z(L)$ , the probabilities  $P_a(t)$  are the solutions of the equation:

$$\frac{d}{dt}P_a(t) = - \sum_b H_{a,b}P_b(t). \quad (3.1)$$

The Hamiltonian  $H$  is an  $Z(L) \times Z(L)$  intensity matrix:  $H_{a,b}$  ( $a \neq b$ ) is non positive and  $\sum_a H_{a,b} = 0$ .  $-H_{a,b}$  ( $a \neq b$ ) is the rate for the transition  $|b\rangle \rightarrow |a\rangle$ . The ground-state wavefunction of the system  $|0\rangle$ ,  $H|0\rangle = 0$ , gives the probabilities in the stationary state:

$$|0\rangle = \sum_a P_a|a\rangle, \quad P_a = \lim_{t \rightarrow \infty} P_a(t). \quad (3.2)$$

In order to go from the discrete time description of the stochastic model to the continuous time limit, we take  $\Delta t = 1/(L - 1)$  and

$$H_{ac} = -r_{ac} \quad (c \neq a), \quad (3.3)$$

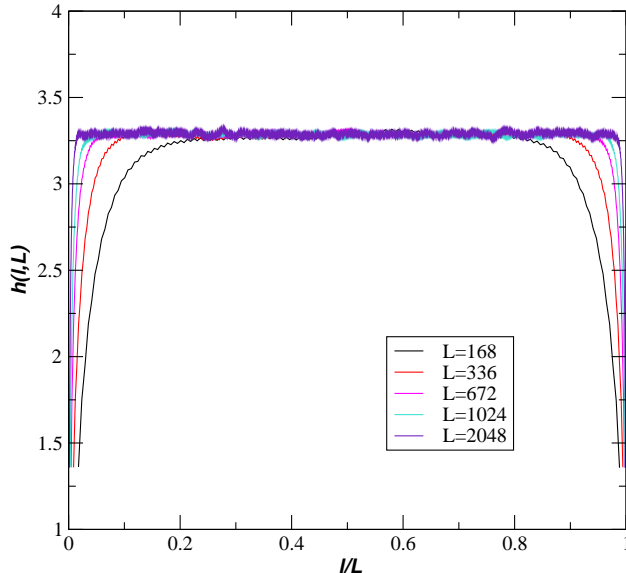


Figure 5: The average height at a site  $l$  for different values of  $L$  in the stationary state of the flip-flop model for  $u = 0.95$  (under the critical point). The lattice sizes are:  $L = 168, 336, 672, 1024$  and  $2048$ .

where  $r_{ac}$  are the rates described above for each of the three models.

## 4 The flip-flop model

We will first discuss the stationary state of the model using some known results in combinatorics. We will discover in this way that we have three phases. One for  $u < 1$ , one for  $u = 1$  and another one for  $u > 1$ . What should we expect to find?

If  $u < 1$ , evaporation takes over deposition of tiles. One should therefore find in the stationary states, in the thermodynamical limit, a finite average height. This assumption is confirmed by Monte Carlo simulations at  $u = 0.95$  for various lattice sizes. The results are shown in Fig. 5. One can observe a constant (site independent) average height. The finiteness of the heights give finite values for the estimators of shared information [14] and therefore we are in a gapped phase.

For  $u = 1$ , all the Dyck paths have the same probability and therefore can be seen as the paths of a restricted random walker who starts at the origin and returns after  $L$  steps. Since it is a random walker, this implies that one is in a gapless phase with a dynamic critical exponent  $z = 2$  [12].

For  $u > 1$ , Dyck paths with large heights are preferred and one can expect a growing interface with  $z = 3/2$  corresponding to the KPZ universality class [4]. In this consideration we didn't take into account the constraints. We are going to see that our guess is not necessarily correct. We proceed by presenting the case  $u > 1$  in detail.

a) *The stationary state.*

It is instructive to take  $L = 6$  and write the Hamiltonian (3.3) in the vector space of the

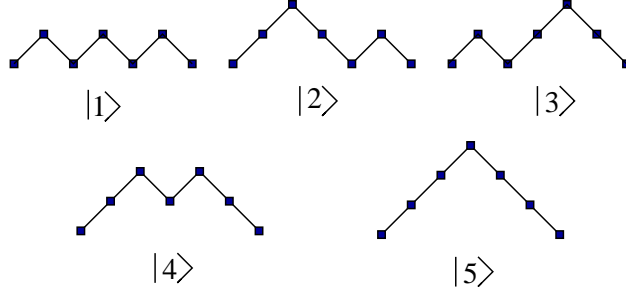


Figure 6: The Dyck path of the  $L = 6$  lattice ( $(L + 1)$  points).

five Dyck paths ( $Z(6) = 5$ ). The five configurations are shown in Fig. 6.

The configuration  $|1\rangle$  corresponds to the substrate. Configuration  $|5\rangle$  in which  $h(L/2, L) = L/2$  is the *pyramid* configuration.

The matrix elements of the Hamiltonian are:

$$H = - \begin{pmatrix} & |1\rangle & |2\rangle & |3\rangle & |4\rangle & |5\rangle \\ \langle 1| & 2u & -1 & -1 & 0 & 0 \\ \langle 2| & -u & 1+u & 0 & -1 & 0 \\ \langle 3| & -u & 0 & 1+u & -1 & 0 \\ \langle 4| & 0 & -u & -u & 2+u & -1 \\ \langle 5| & 0 & 0 & 0 & -u & 1 \end{pmatrix}. \quad (4.1)$$

The wavefunction corresponding to the eigenvalue zero is:

$$|1\rangle + u|2\rangle + u|3\rangle + u^2|4\rangle + u^3|5\rangle. \quad (4.2)$$

Notice that in the stationary state wavefunction each configuration gets as a coefficient a monomial in  $u$  with an exponent equal to the number of tiles on the top of the substrate. We have chosen the coefficient of the substrate (no tiles) to be equal to one. For large values of  $u$ , the configuration  $|5\rangle$  corresponding to the *pyramid* is preferred, for small values of  $u$ , the configuration  $|1\rangle$ , which corresponds to the substrate has the largest probability. The normalization factor

$$Z_6(u) = 1 + 2u + u^2 + u^3 \quad (4.3)$$

is equal to the generating function for the number of tiles. One can easily check that this observation is valid for any number of sites and that the normalization factor  $Z_L(u)$  is the generating function for the number of tiles for any lattice size  $L$ . Once this point is made, one can use results from combinatorics to get the phase diagram of the model.

It turns out [15] that  $Z_L(u)$  is related to the Carlitz  $q$ -Catalan numbers  $C_n(q)$  ( $L = 2n$ ). The latter are defined by the recurrence relations:

$$C_{n+1}(q) = \sum_{k=0}^n C_k C_{n-k} q^{(k+1)(n-k)}, \quad (C_0 = 1). \quad (4.4)$$

We give the first ones:

$$\begin{aligned} C_1 &= 1, & C_2 &= 1 + q, & C_3 &= 1 + q + 2q^2 + q^3, \\ C_4 &= 1 + q + 2q^2 + 3q^3 + 3q^4 + 3q^5 + q^6. \end{aligned} \quad (4.5)$$

One can define another deformation of the Catalan numbers

$$\tilde{C}_n(u) = u^{\frac{n(n-1)}{2}} C_n(u^{-1}), \quad (4.6)$$

which are the solutions of the recurrence relations

$$\tilde{C}_{n+1}(u) = \sum_{k=0}^n u^k \tilde{C}_k(u) \tilde{C}_{n-k}(u), \quad (\tilde{C}_0 = 1). \quad (4.7)$$

One has

$$Z_L(u) = \tilde{C}_n(u) \quad (L = 2n). \quad (4.8)$$

The average number of tiles is

$$N_L(u) = u \frac{d}{du} \ln Z_L(u). \quad (4.9)$$

There is no known explicit expression for  $Z_L(u)$  for finite values of  $L$  and its asymptotics is known only for  $u > 1$  [15]:

$$\lim_{n \rightarrow \infty} Z_{2n}(u) = u^{\frac{n(n-1)}{2}} / \phi(u^{-1}), \quad (4.10)$$

where  $\phi(q)$  is the Euler function

$$\phi(q) = \prod_{n=1}^{\infty} (1 - q^n). \quad (4.11)$$

Using (4.9) and (4.10) one can compute the average number of tiles in the large  $L$  limit. One gets

$$\lim_{L \rightarrow \infty} N_L(u) = \frac{n(n-1)}{2} + C(u), \quad (4.12)$$

where the  $L$ -independent term  $C(u)$  is:

$$C(u) = - \sum_{k=1}^{\infty} \frac{k}{u^k - 1}. \quad (4.13)$$

It follows that the average number of tiles is equal to those in the pyramid  $n(n-1)/2$  for any  $u!$  As a consequence, the dominant configurations are those close to the full "pyramid" for any  $u > 1$ . Monte Carlo simulations for finite values of  $L$  confirm this result. Taking  $u = 1.05$  we show in Fig. 7a some typical heights profiles for several lattice sizes and in Fig. 7b the average values of the heights. One sees that with increasing values of  $L$ , one reaches the "pyramid" configuration.

In the Appendix we consider a model in which the adsorption and desorption processes are the same as in the flip-flop model but the configuration space is not anymore Dyck paths, the constraint (2.3) being relaxed. In the large  $L$  limit, the physics is the same as the one observed in the flip-flop model for  $u > 1$ .

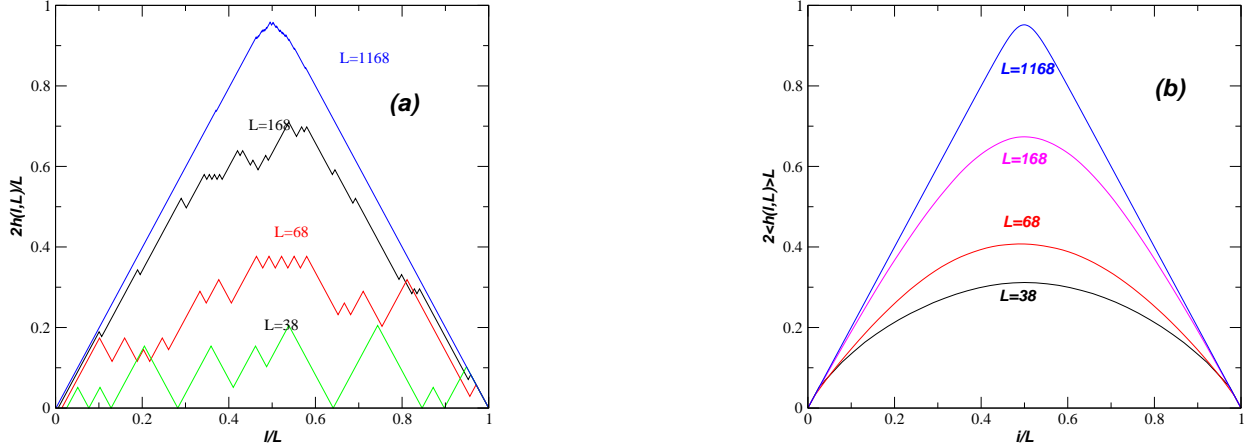
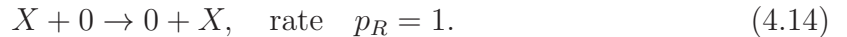


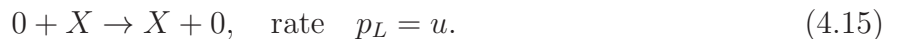
Figure 7: a) Typical configurations of the heights  $h(l, L)$  (multiplied by  $2/L$ ) in the flip-flop model for  $u = 1.05$  (over the critical point) and different system sizes ( $L = 38, 68, 168$  and  $1168$ ). For the pyramid configuration,  $2h(L/2)/L = 1$ . b) Average values, considering  $10^5$  configurations for the same systems in (a).

One expects that the whole  $u > 1$  domain to be gapped and that for any initial condition, the systems evolve fast to reach the configurations closed to the full pyramid. We are going to show below that this is indeed the case.

One can understand this result in a different way by using the *Dyck paths*  $\rightarrow$  *particle* mapping. The desorption process *peak*  $\rightarrow$  *valley* with a rate one is mapped in the hopping of a particle to the right:



The adsorption process *valley*  $\rightarrow$  *peak* with a rate  $u$  is mapped in the hopping to the left:



We have to take the two constraints into account. The system is confined to the size  $L$  and the number of particles to the left of each bond has to be larger than the number of vacancies. One can consider ASEP with boundaries [1] and try to mimic the constraint by injecting with a large rate  $\alpha$  particles on the first site and removing particles with a rate  $\beta = \alpha$  (the density of particles has to be equal to the number of vacancies). This picture should be correct if  $p_L > p_R$  ( $u > 1$ ) when one has a reverse bias. The partition function was computed [16] and one obtains for large systems, a factor  $u^{n^2/16}$ , similar to Eq. (4.10). In both cases the exponent is an area and not a length. The current also vanishes in this limit. There is no current in our model.

This mapping gives absurd results if  $u < 1$  ( $p_R > p_L$ ). Since we have equal densities, in ASEP with boundaries we are in the maximum current phase which is gapless. In our model there is no current, there are no density fluctuations and one is gapped.

To sum up, the study of the stationary state suggests the following phase diagram for the flip-flop model. It has a gapped phase for  $u < 1$ , is gapless at  $u = 1$  with  $z = 2$  and gapped for  $u > 1$ . We now show that the time evolution results confirm this picture.

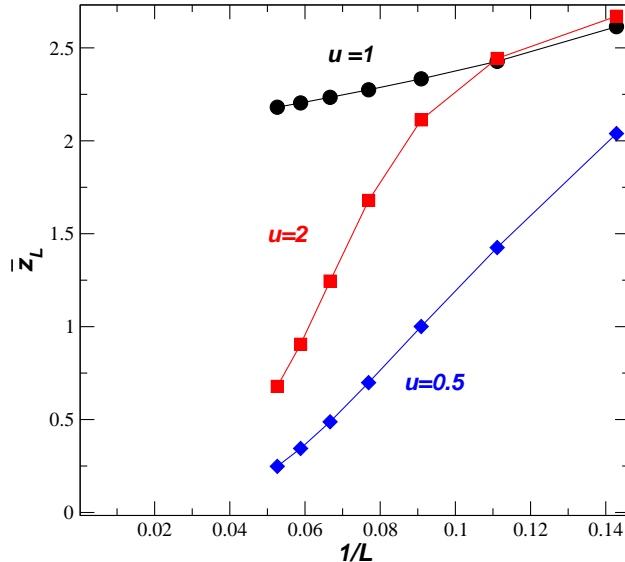


Figure 8: Estimates of the dynamic critical exponent  $z$  using (4.17), as a function of  $1/L$ , in the three phases.

b) *Gaps and the dynamical critical exponent  $z$*

In order to see which phases are gapped or gapless, we have diagonalized numerically (up to  $L = 18$ ) the Hamiltonian (3.3) for the FFM. Since the lowest energy is zero (the Hamiltonian describes a stochastic process), the energy gap is given by the first excited state  $E_1(L)$ . One expects

$$E_1(L) = a_1 L^{-z}, \quad (4.16)$$

where  $z$  is the dynamical critical exponent and  $a_1$  a constant. A value  $z = 0$  implies that the system is gapped. In Fig. 8 we show the estimates for  $z$  defined as

$$\bar{z}_L = \ln \left( \frac{E_1(L)}{E_1(L-2)} \right) / \ln \left( \frac{L-1}{L} \right), \quad (4.17)$$

up to  $L = 18$ , in the three phases. One sees that  $\bar{z}_L$ , as expected, goes towards the value 2 for  $u = 1$  and to zero in the other two phases. To sum up, the phase diagram of the flip-flop model is as follows:

$$u < 1 \quad \text{gapped}, \quad u = 1 \quad \text{gapless} \quad (z = 2), \quad u > 1 \quad \text{gapped}. \quad (4.18)$$

A version of the flip-flop model in which the rates are the same, but with a configuration space without the constraint (2.3), is presented in Appendix A.

## 5 The raise and peel model - some results

As a result of the changes occurring in the adsorption process which is nonlocal as compared to the FFM where it is local, the physical properties of the phases in the same phase diagram

also change. Like in the FFM, the  $u < 1$  domain is gapped. Instead of a  $z = 2$  phase transition, at  $u = 1$  one has a  $z = 1$  phase transition with a space-time symmetry (conformal invariance). For  $u > 1$ , the system stays gapless with varying dynamic critical exponents  $z$  ( $z$  decreases when  $u$  increases) and is not gapped like in the FFM.

Since in the RSM we will find again a  $z = 1$  phase transition with conformal invariance, we will sum up the main results obtained in the RPM at  $u = 1$  [7] in order to compare them in the next sections with those which will be seen in the RSM.

First we discuss the stationary state. In the finite-size scaling limit  $l, L \gg 1$ ,  $l/L$  fixed, the average height at a distance  $l$  from the origin, for a system of size  $L$ , has the expression:

$$h(l, L) = \frac{\sqrt{3}}{2\pi} \ln L_c, \quad (5.1)$$

where

$$L_c = \frac{L}{\pi} \sin\left(\frac{\pi l}{L}\right). \quad (5.2)$$

We would like to mention that for  $u > 1$ , similar to (5.1),  $h(l, L)$  shows a logarithmic increase with the size of the system  $L$  but with a different dependence on  $l/L$ .

The density of contact points in the same limit, has the expression

$$g(l, L) = \frac{\alpha}{L_c^{1/3}} \quad (5.3)$$

with

$$\alpha = -\frac{\sqrt{3}\Gamma(-1/6)}{6\pi^{5/6}} = 0.753149\dots \quad (5.4)$$

These expressions are exact. Notice the logarithmic growth of the interface and that the lengths dependence is all in  $L_c$ . The latter is a consequence of conformal invariance.

For  $u < 1$ , in the vicinity of the critical point  $u = 1$ , and large values of  $L$ , the average density of clusters  $K(u)$  is  $L$  independent and vanishes like

$$K(u) = 0.596(1 - u)^{0.78}. \quad (5.5)$$

This result is new. It was obtained using Monte Carlo simulations. This result is a surprise. The scaling dimensions in the model are  $1/3$  and  $1$  [17] and no combination of them can give a number close to the exponent  $0.78$ .

The average density of peaks and valleys, in the large  $L$  limit, is

$$\tau = \frac{3}{4}. \quad (5.6)$$

The physical meaning of (5.6) is the following one. Adsorption takes place only on valleys which occupy a  $3/8$ th fraction of the number of sites, whereas desorption takes place on a  $2/8$ th fraction of the number of sites. Since in a desorption process one loses more tiles than one gains in an adsorption process, one needs more sites with valleys than sites where

desorption can take place. In the RPM peaks are not active. This picture will change in the RSM in which sites with both valleys and peaks are active.

The spectrum of the Hamiltonian (3.3), in the finite-size scaling limit, is given by

$$\lim_{L \rightarrow \infty} E_i(L) = \frac{\pi v_s}{L} \Delta_i, \quad i = 0, 1, 2, \dots, \quad (5.7)$$

where  $E_0 = 0$ ,  $\Delta_i$  are the scaling dimensions and the sound velocity  $v_s$  has the value

$$v_s = \frac{3\sqrt{3}}{2}. \quad (5.8)$$

The scaling dimensions  $\Delta_i$  and their degeneracies ( $d_i$ ) can be obtained from the partition function [17]

$$Z(q) = \sum_{i=0} q^{\Delta_i} = (1-q) \prod_{n=1}^{\infty} (1-q^n)^{-1}. \quad (5.9)$$

We give the first values of  $\Delta_i$  and  $d_i$ :

$$\Delta = 0(1), 2(1), 3(1), 4(2), \dots \quad (5.10)$$

As we are going to see in the next Section, the RSM has a phase diagram similar to the RPM. For  $u < u_c$  the system is gapped, at  $u = u_c$  it is conformal invariant and gapless for  $u > u_c$  with varying dynamical critical exponent  $z$ . The value of  $u_c$  being not equal to one anymore. Which properties described above should one expect at  $u_c$ ?

In the stationary state, the  $l$  and  $L$  dependence in the finite-size limit of the average density of contact points and heights should be again through the function  $L_c$  given by (5.2). The exponents might be different. How about the spectrum of the Hamiltonian (3.3)? Since the scaling dimension  $\Delta_1 = 2$  corresponds to the energy-momentum tensor, it should be not degenerate. The other values of  $\Delta_i$  should be present but they might have other degeneracies.

Using  $E_1(L)$  and (5.7) with  $\Delta_1 = 2$ , one can determine  $v_s$ . The ratios  $E_i(L)/E_1(L)$  should be equal to  $n/L$  ( $n = 3, 4, \dots$ ) for large  $L$ .

## 6 The raise and strip model

We are going to show that this model has a phase diagram similar to those found in the previous two models. A gapped phase for  $u < u_c$ , a critical point at  $u_c$  and a new gapless phase for  $u > u_c$ . In establishing the phase diagram one encounters a new problem:  $u_c$  is not known exactly and one has to take care of possible cross-over effects.

We have analyzed, using Monte Carlo simulations, the heights profiles for different values of  $u$  and lattice sizes and found that up to  $u$  around 4.5 they are flat and the average height is  $L$  independent for large values of  $L$ , suggesting a gapped phase. In Fig. 9 we show for  $u = 3$ , the  $L$  dependence of  $h(L/2, L)$ , the average height in the middle of the system. One sees that its value saturates fast with increasing values of  $L$ .

The values of the average heights are larger than those observed in the RPM. For larger values of  $u$  there is a sharp increase of the height in the middle of the system. In Fig. 10

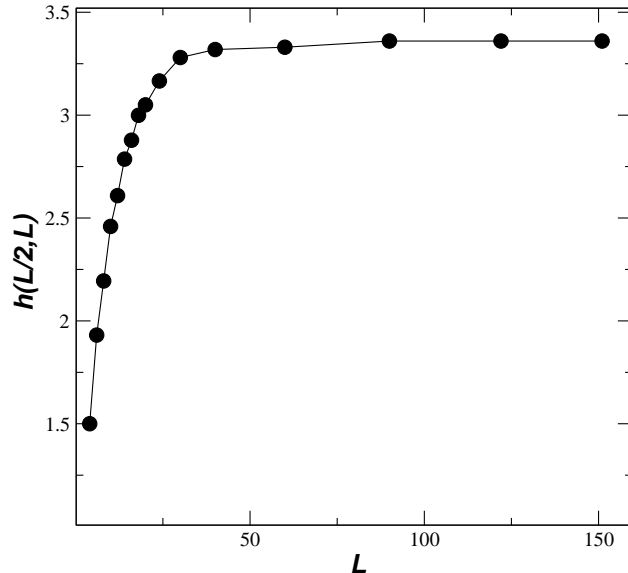


Figure 9: The RSM. The height in the middle of the system  $h(L/2, L)$  for  $u = 3$  as a function of  $L$ . The results were obtained by averaging  $10^8$  samples. The estimated errors are smaller than the symbols representing the data.

we show the heights profiles in the domain  $4.5 \leq u \leq 5.4$  for  $L = 2048$ . One sees that for  $u = 5.4$  one sees almost a triangle with a rounded tip. A similar triangle was seen in the flip-flop model in the  $u > 1$  domain. There is however a major difference between the triangles observed in the two models. Whereas in the FFM the triangle coincides with the pyramid configuration for which the height in the middle is equal to  $L/2$ , for  $u = 5.4$  in the RSM the average height in the middle is around 30% of  $L/2 = 1024$ . If one considers larger values of  $u$  the height of the triangle increases but never reaches the pyramid's height. These observations suggest the existence of a new phase in which the system grows linearly with the size of the system. We will denote this phase by LG (linear growth). We will learn more about it below.

A closer inspection of the interval  $4.6 \leq u \leq 4.7$  suggests a phase transition between the gapped phase and the LG phase. In this interval the profiles are not sharp at the boundaries as in the gapped phase (one has an exponential fall-off in this case) and the height at the profile is not a triangle. One expects therefore  $u_c$  to be in this interval.

We proceed now to a detailed analysis of the model. There is not much to say about the gapped phase. As we are going to show below, a good estimate for  $u_c$  is  $u_c = 4.685$ . We have measured using Monte Carlo simulations the density of clusters in the gapped phase and found for  $u$  close to  $u_c$

$$K(u) = 0.035(4.685 - u)^{1.733}. \quad (6.1)$$

This expression is quite different of the one observed for the RPM (5.5). There are fewer contact points in the gapped phase in the RSM than in the RPM. This is consistent with the observation that the heights in the gapped phase are higher in the RSM than in the RPM.

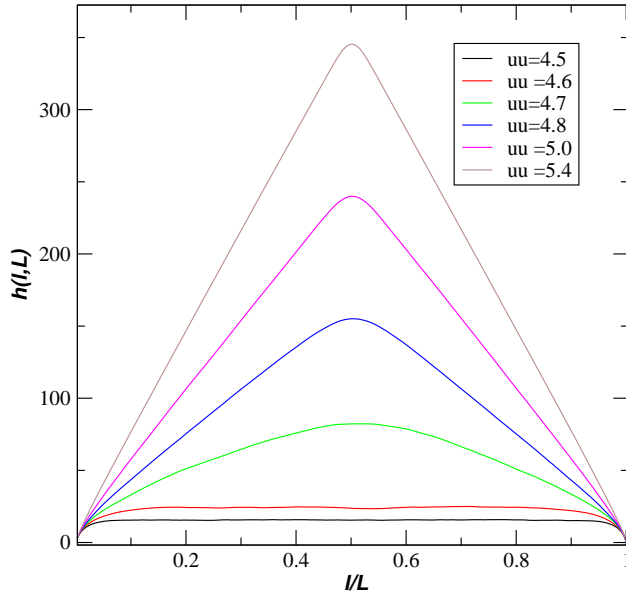


Figure 10: Average height  $h(l, L)$  as a function of  $l$  in the RSM for various values of  $u$ : 4.5, 4.6, 4.7, 4.8, 5.0 and 5.4. The size of the system is  $L = 2048$ . The average is taken over  $10^8$  independent samples.

We first discuss the  $u_c$  physics and show that we have conformal invariance for this value of  $u$ . We present the results for the stationary state and time dependent observables. The LG phase is going to be discussed afterwards.

a) *The stationary state at  $u_c$ . Conformal invariance.*

We consider the density of contact points  $g(l, L)$  for various values of  $u$  in the interval where we suspect to have the phase transition. If we have conformal invariance (see Section 5), we should have in the finite-size scaling limit

$$g(l, L) = C_g L_c^{-\mu}, \quad (6.2)$$

where  $L_c$  is given by (5.2),  $C_g$  is a constant and  $\mu$  a critical exponent to be determined. The results of the Monte Carlo simulations are presented in Fig. 11 for  $L = 4096$ . It is shown that for  $u = 4.685$  one obtains a very nice fit to the data if one takes:

$$g(l, L) = 1.26 L_c^{-1.65}. \quad (6.3)$$

Notice that the value of  $\mu$  is very closed to  $5/3$ .

One can have a different look at the data for  $u_c = 4.685$  and  $L = 4096$  (see Fig. 12) plotting  $g(l, L) \times L_c^{1.667}$  as a function of  $\sin(\pi l/L)$ . One observes that within the errors, one obtains a constant, as expected. We have to stress that there is a small drift in the estimates of  $u_c$  with the size of the system. If one uses the  $L = 2048$  data, the value  $u_c = 4.681$  is preferred. This observation is illustrated in Fig. 13.

The next quantity we are looking at is the average height  $h(l, L)$ . If we have conformal invariance, in the finite-size limit we expect to find the expression:

$$h(l, L) = C_h L_c^\nu, \quad (6.4)$$

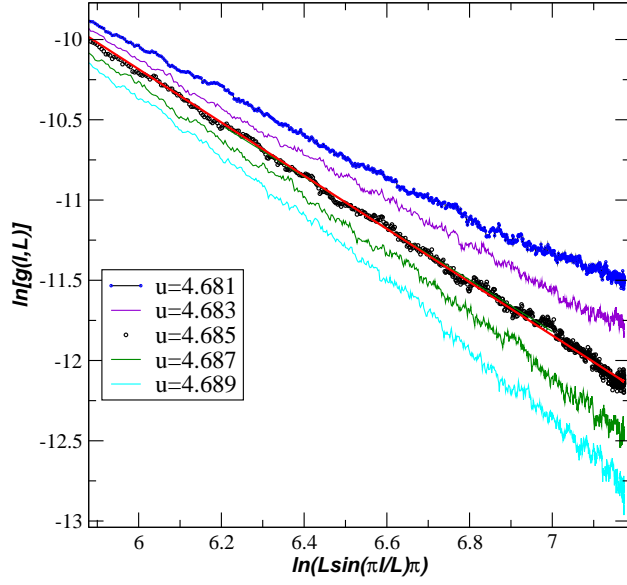


Figure 11:  $\ln[g(l, L)]$  in the RSM as a function of  $L_c$  for  $L = 4096$  and for the values of:  $u = 4.681, 4.682, \dots, 4.689$ . The results are obtained by averaging over  $10^9$  Monte Carlo steps. The fitting curve at  $u = 4.685$  is  $y = -0.234 - 1.65x$ .

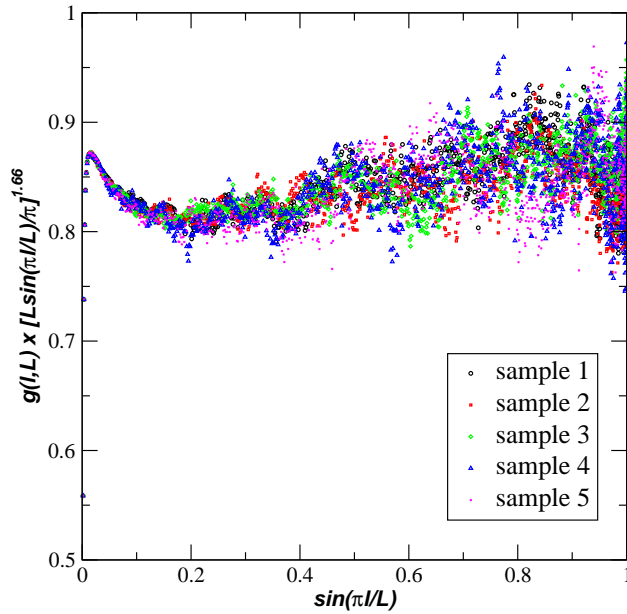


Figure 12: The density of contact points  $g(x, L)$  multiplied by  $(L_c)^{1.66}$  as a function of  $\sin(\pi/L)$  for  $u = 4.685$  and  $L = 4096$ . We show the results of five samples with  $10^9$  Monte Carlo steps

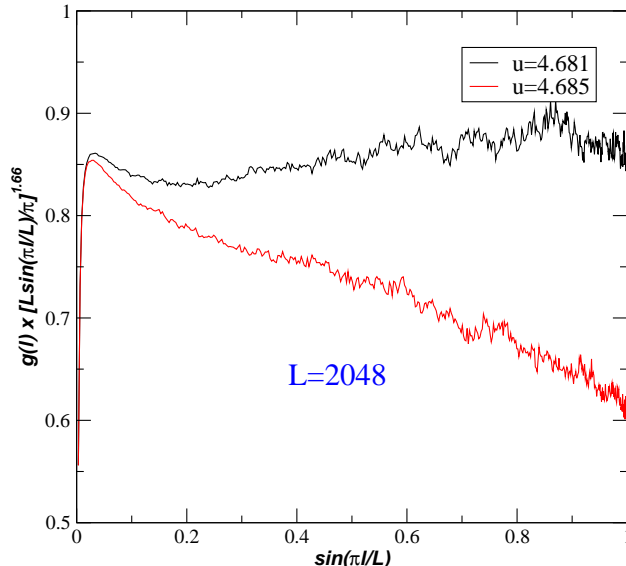


Figure 13: Effect of the lattice size on the determination of  $u_c$  for the lattice size  $L = 2048$  by averaging  $10^9$  Monte Carlo steps. The value  $u_c = 4.681$  gives a better estimate for  $u_c$  than  $u_c = 4.685$  obtained for  $L = 4096$ .

where  $\nu$  is a critical exponent and  $C_h$  is a constant. Using the data obtained for  $u_c = 4.685$  in Fig. 14 we plot  $h(l, L) \times L_c^{0.5}$  as a function of  $\sin(\pi l/L)$  and find almost a constant value. This implies  $\nu = 0.5$ . We have measured  $\nu$  considering  $h(L/2, L)$  for various values of  $L$  and our best estimates are  $0.50 \leq \nu \leq 0.52$ . An exact estimate for  $\nu$  is hard to get since, as mentioned above, the estimates of  $u_c$  change slightly with  $L$ .

Finally one has measured the density of peaks and valleys for large values of  $L$  and obtained

$$\tau \approx 0.35. \quad (6.5)$$

What have we learned up to now about the  $u_c$  phase transition? The data are compatible with conformal invariance. We will also show below that the critical exponent  $z = 1$  and that the spectrum of the Hamiltonian is what we expect. Although they are both conformal invariant, the phase transitions at  $u = 1$  for the RPM and at  $u_c$  for the RSM are different. The average height growth logarithmically in the RPM and like a power in the RSM. The density of contact points has an exponent  $1/3$  in the RPM and probably  $5/3$  in the RSM. Also the density of peaks and valleys are different. There are fewer peaks and valleys in the RSM. This can be understood as follows: since the phase transition takes place at a large value of  $u$ , in the stationary state, many tiles are adsorbed therefore many have to be desorbed. This implies that one needs many sites without peaks or valleys.

b) *Time dependent phenomena at  $u_c$ .*

In order to determine the value of the dynamic critical exponent  $z$ , we use the properties of the Family-Vicsek scaling function [18]. We first consider the density of clusters  $K(L, t)$ . From (6.3) follows that the number of clusters is finite therefore the density of clusters in the stationary state behaves like

$$K(L) = C_K/L, \quad (6.6)$$

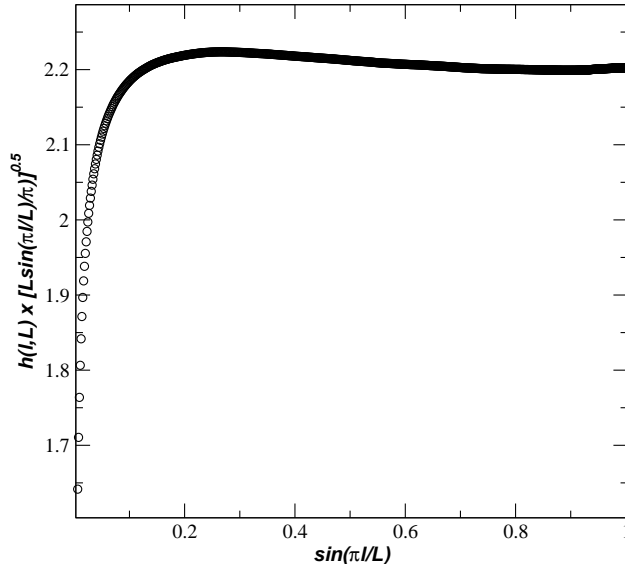


Figure 14: The average height  $h(l, L)$  multiplied by  $L_c^{1/2}$  as a function of  $\sin(\pi l/L)$  for  $u = 4.685$  and  $L = 4096$ . The results shown are obtained by averaging  $10^9$  Monte Carlo steps. The estimated error are smaller than the symbols in the figure.

where  $C_K$  is a constant. This implies that for large values of  $L$  and short times one expects

$$K(t) = \frac{D_K}{t^{1/z}}, \quad (6.7)$$

being  $D_K$  a constant. In Fig. 15 we show the short time dependence of  $K(t)$ , and a fit to the data gives

$$\ln[K(t)] = -1.38 - 0.99 \ln(t), \quad (6.8)$$

from which we get the value  $z = 1.01$  extremely close to the value  $z = 1$  required by conformal invariance.

A similar analysis was done for the average height at the half value of  $L$ ,  $h(L/2, L)$ . Since in the stationary state  $h(L/2, L) \approx L^{1/2}$ , we expect, if  $z = 1$  that for short times and large values of  $L$  to find  $h(L/2, L, t) \approx t^{1/2}$ . This expectation is confirmed by the data shown in Fig. 16, where for short times the fit gives:

$$\ln[h(L/2, L, t)] = 0.154 + 0.49 \ln(t). \quad (6.9)$$

A final confirmation of conformal invariance at  $u_c$  is obtained looking at the first excited states of the Hamiltonian (3.3) at  $u_c = 4.685$ . We have diagonalized numerically the Hamiltonian up to  $L = 18$ . In Fig. 17 we show for convenience  $L \times E_1(L)/2\pi$  and not  $L \times E_1(L)/\pi$  as a function of  $1/L$ . Using the data and (5.7) with  $\Delta = 2$  one gets  $v_s \approx 3.7$  (a value of the same order as the value (5.8) in the RPM). We also show the ratios  $E_2(L)/E_1(L)$  and  $E_3(L)/E_1(L)$ , as a function of  $L$ . The data nicely converge to the value  $3/2$  indicating that we have two levels with  $\Delta = 3$  (in the RPM one has only one level with this value, see (5.10)).

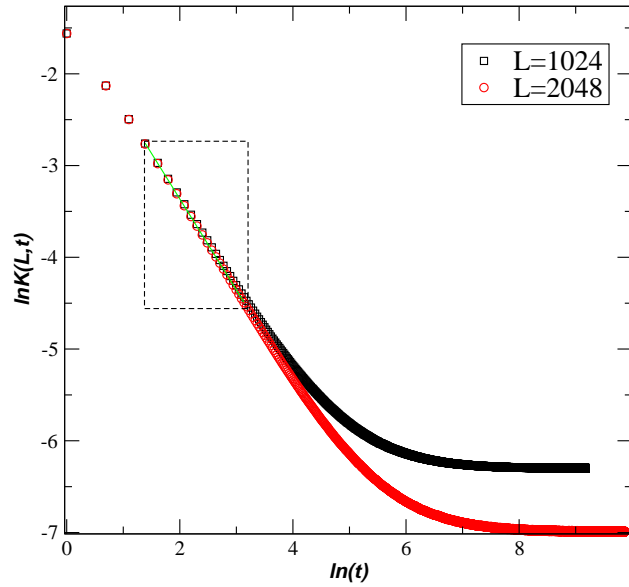


Figure 15: Determination of the dynamic critical exponent  $z$  at  $u = 4.685$ . The density of clusters versus time on a log scale. The substrate was used as the initial condition, and the average was taken over  $10^6$  samples. The fitting  $y = -1.38 - 0.99x$  was obtained in the region inside the dashed box.

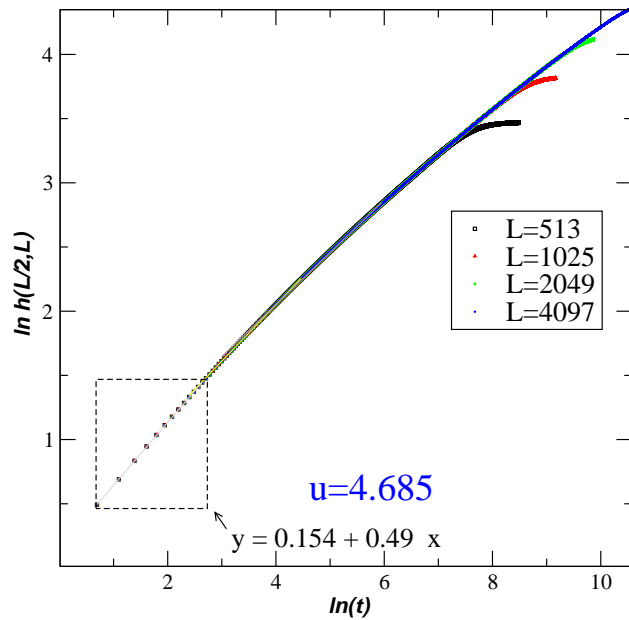


Figure 16: The average height at  $L/2$  as a function of time for  $L = 512, 1024, 2048, 4096$  on log scales. The initial state was the substrate, and the average was over  $10^6$  samples. The region where the fitting was taken is also shown.

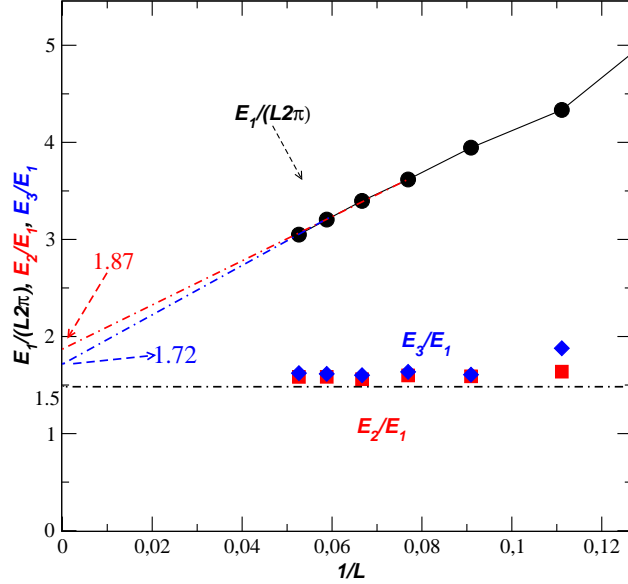


Figure 17: Finite-size scaling analysis of the spectrum of the Hamiltonian at  $u_c = 4.685$ . The data are obtained by diagonalizing the Hamiltonian up to 18 sites.  $LE_1(L)/2\pi$ ,  $E_2(L)/E_1(L)$  and  $E_3(L)/E_1(L)$  are shown as a function of  $1/L$ . The extrapolated values for  $E_1/(2\pi L)$  is also shown.

The existence of two levels with  $\Delta = 3$  is a puzzle. Since the central charge of the Virasoro algebra is  $c = 0$  (for a stochastic model the ground state of the Hamiltonian is always equal to zero), the character corresponding to the vacuum representation is  $\chi_0(q) = Z(q)$  (see (5.9)). There is only one scaling dimension with  $\Delta = 3$  (see (5.10)). On the other hand,  $\Delta = 3$  is not in the Kac table according to which the scaling dimensions are

$$\Delta_{r,s} = [(3r - 2s)^2 - 1]/24 \quad (6.10)$$

with  $r$  and  $s$  positive integers and therefore one has to add to the spectrum a standard Virasoro character:

$$\chi_3(q) = q^3 \prod_{n=1}^{\infty} (1 - q^n)^{-1}. \quad (6.11)$$

In the finite-size scaling limit, the spectrum of the Hamiltonian is given by the partition function  $\chi_0(q) + \chi_3(q)$ . This implies the following values of  $\Delta_i$  and degeneracies ( $d_i$ ):

$$\Delta = 0(1), \quad 2(1), \quad 3(2), \quad 4(3), \quad 5(4), \quad \dots \quad (6.12)$$

In order to check if the levels with the corresponding degeneracies are seen in our model, we have looked at the lower part of the spectrum of the Hamiltonian for  $L = 18$ . Normalizing the eigenvalues by taking  $E_1(18) = 2$ , one gets the following values:

$$0; \quad 2; \quad 3.16; 3.24; \quad 4.35; 4.36; 4.54; \quad 5.20; 5.4; 5.6; 6.0; \dots \quad (6.13)$$

We have checked that the values of  $E_i(L)/E_1(L)$  converge from above from larger values and cluster towards their asymptotic ones. We conclude that, although the lattice sizes are up

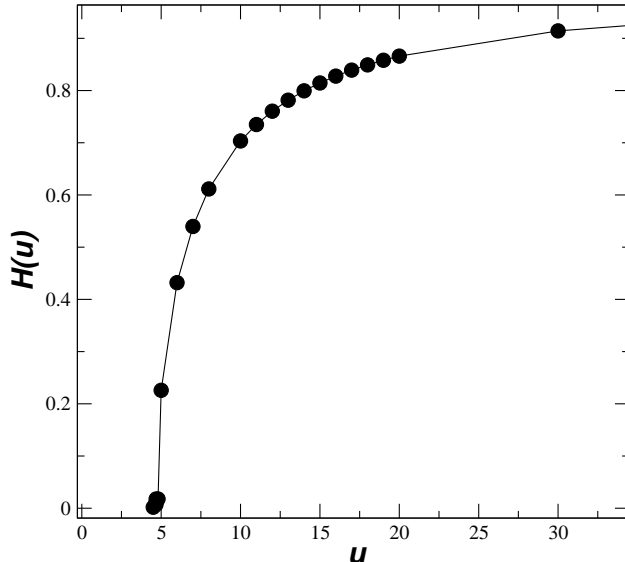


Figure 18: The  $u$  dependence of  $H(u)$ . Monte Carlo simulations for lattice  $L = 16384$ . The results were obtained by taking  $10^7$  Monte Carlo steps. The estimated errors are smaller than the symbols.

to  $L = 18$ , at least for the lower part of the spectrum there is agreement between (6.13) and (6.12).

We have tried to see if at  $u_c$ , the Hamiltonian has hidden symmetries for finite  $L$ . They could show up in the observation of degeneracies of the spectra at finite  $L$ . In (6.13) one notices that two couples of values are very close (3.16 and 3.24 respectively 4.35 and 4.36). Since  $u_c$  is not known exactly we have checked if small changes in the value of  $u$  around the value 4.685 could make the levels degenerate for all values of  $L$ . Our investigation gave a negative result. Degeneracies were observed only for one of the two couples and only for one value of  $L$ . This observation probably excludes the existence of Jordan cells in the finite-size scaling limit since in all known examples the Jordan cells occurring in the conformal theory appear already for finite values of  $L$ .

c) *The linear growth phase ( $u > u_c$ ).*

As mentioned earlier, in this phase the heights profiles in the stationary state are triangles (see Fig. 10 for  $L = 2048$ ) with heights which are fractions of the maximum possible height  $L/2$ . The maximum height is seen in the stationary states of the FFM. We have studied the  $u$  dependence of

$$H(u) = 2h(L/2, L)/L \quad (6.14)$$

using Monte Carlo simulations for a very large lattice ( $L = 16384$ ). The results are shown in Fig. 18. One notices, as expected, that  $H(u)$  increases with  $u$  (for  $u$  infinite,  $H(u) = 1$ , the triangle becomes the pyramid).

Since  $H(u)$  has a clear geometrical meaning, it can be seen as an order parameter in the LG phase [19].

In order to determine the values of the dynamic critical exponent  $z$ , we have performed an analysis similar to the one done for  $u = u_c$  (see eqs. (6.6) and (6.7)). We have first convinced

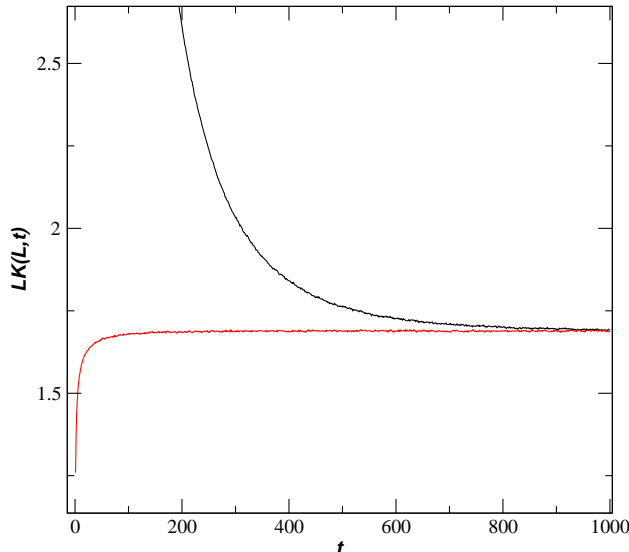


Figure 19: The number of clusters  $LK(L, t)$  as a function of time for two different initial conditions (pyramid in red and substrate in black). The lattice size is  $L = 4096$  and  $u = 5$ . On each evolution there were  $4 \times 10^5$  samples in the Monte Carlo simulations.

ourselves that for  $u > 1$  in the stationary state and the large  $L$  limit the number of clusters stays finite. Starting with two different configurations (the substrate and the pyramid), we have looked at the time dependence of the number of clusters  $C_K(t)$  and checked if they converge at the same value  $C_K$ . The results of the computer simulations for  $L = 4096$  and  $u = 5$  shown in Fig. 19 show that this is indeed the case. This observation implies that in the stationary state, the density of clusters is given by eq. (6.6). The next step is to determine  $z$  using eq. (6.7).

In Fig. 20 we show the short time dependence of the density of clusters for various lattice sizes and  $u = 7$ . One has used the substrate as initial condition. Notice the data collapse which allows to determine  $z$ . A similar analysis was done for other values of  $u$ . Our estimates for  $z$  are 0.77 ( $u = 5.5$ ), 0.66 ( $u = 6$ ), 0.5 ( $u = 7$ ), 0.43 ( $u = 8$ ), 0.35 ( $u = 10$ ).

We conclude that in the LG phase one is gapless, the dynamic critical exponents decrease in value with increasing values of  $u$ . We had a similar behavior in the RPM.

## 7 Conclusions

We have considered three one-parameter dependent stochastic models (FFM, RPM and RSM) defined on Dyck paths. Dyck paths have fixed boundaries (2.2) and are confined to the upper half plane (2.3). The parameter denoted by  $u$  in the text, is equal to the ratio of the adsorption and desorption rates. Adsorption is local in the three models, desorption is local in the FFM and nonlocal in the other two. The phase diagrams of the three models are similar: for  $u < u_c$  the model is gapped, it undergoes a phase transition at  $u_c$  where it is gapless, for  $u > u_c$  it is again gapped for the FFM but gapless for the RPM and RSM in which desorption is nonlocal.

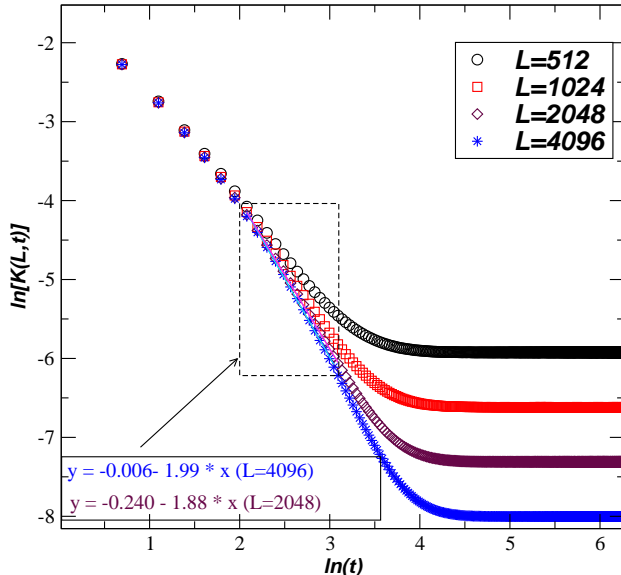


Figure 20: Short time dependence of the density of clusters for several lattice sizes of the RSM at  $u = 7$ . It is also shown the fitting results in the region of the dashed rectangle for  $L = 2048$  and  $L = 4096$ . On each evolution there were  $4 \times 10^5$  samples in the Monte Carlo simulation.

The aim of the paper was to understand the effect of having nonlocal rates. The raise and peel model was shortly described here because it is, as far as we know, the first intensively studied model [5,6] in which the desorption process, which takes place when a tile hits a slope, is nonlocal. The peaks are not active. In the raise and strip model presented for the first time in this paper, the slopes are not active but when a tile hits a peak it triggers a nonlocal desorption process. In order to clarify the role of nonlocality in the latter model, we have presented the flip-flop model which is similar to the RSM (the peaks and valleys are the active sites) with the major difference that desorption is local.

Two Dyck paths play an important role in these models: the substrate (no tiles) and the pyramid configuration in which the height at the middle is equal to half the size of the system. If  $u = 0$ , the stationary state is the substrate configuration in all three models.

In the flip-flop model  $u_c = 1$  and the dynamical critical exponent  $z = 2$  (one has a random walker). We have studied the spectra of the Hamiltonian for  $u < 1$  and  $u > 1$  and obtained that the system is gapped in both cases. In the stationary state, the average height is finite for  $u < 1$ , and increases like  $L^{1/2}$  at  $u = 1$  ( $L$  is the system size). For any  $u > 1$ , in the large  $L$  limit, the system has small fluctuations around the pyramid configuration (the average height at the middle of the system  $h(L/2, L)$  is equal to  $L/2$ ). This result was obtained using known results from combinatorics. A variant of this model in which the configuration space is changed (RSOS paths without the restriction (2.3)) and the rates are local is presented in Appendix A. The results are similar to those obtained for the flip-flop model.

In the raise and peel model,  $u_c = 1$ , the dynamical critical exponent  $z = 1$  and one has conformal invariance. It is this special property which inspired our work presented here. Is conformal invariance a consequence of nonlocality? That this might be the case is suggested

by the observation that in the peak adjusted raise and peel model [11] where adsorption is also nonlocal, one has conformal invariance. In the stationary states the average heights are finite for  $u < 1$  and increase logarithmically with  $L$  not only for  $u = 1$  but also for  $u > 1$ . There are many properties of this model which are known exactly because the Hamiltonian is integrable at  $u = u_c = 1$ .

The raise and strip model is most probably not integrable. All our results are based on Monte Carlo simulations on large lattices. The best estimate for the critical point is  $u_c = 4.685$ . For  $u < u_c$  and large  $L$ , the average values of the heights stay finite albeit larger than in the RPM. For  $u = u_c$ , one obtains  $z = 0.99$  very close to the value  $z = 1$ . Several tests suggest that one has conformal invariance. At  $u_c$  the RSM model has different properties than the RPM. The finite-size scaling spectrum of the Hamiltonian are given by different Virasoro modules in the two models. The critical exponents are also different. The average height increases like a power of  $L$  and not like  $\ln L$ . For  $u > u_c$  the dynamical critical exponent  $z$  decreases if  $u$  increases, similar to what was observed in the RPM. The analogy stops here however. Whereas in the RPM the average height increases logarithmically with  $L$ , in the RSM the heights profile is very different. For large values of  $L$ , the profile is a triangle with the tip increasing linearly with  $L$ . We have therefore called this domain of  $u$ , the "linear growth phase". For  $u$  very large the triangle gets close to the pyramid configuration seen in the flip-flop model.

We believe that the phase diagram observed in the RPM and RSM is general for the class of models of nonlocal growth. This has of course to be proven looking at other models. Such a study might also bring a better understanding of some properties of the RSM (the values of the exponents are just one example).

The relevance of our work for physical systems like polymers with nonlocal interactions [21, 22, 23] remains to be studied.

## 8 Acknowledgments

We would like to thank A. Gainutdinov for suggesting Eq. (6.12), B. Derrida, H. Hinrichsen and V. B. Priezzhev for discussions. This work was supported in part by FAPESP and CNPq (Brazilian Agencies).

## A Filling a square with tiles

This is the flip-flop model described in Section 3 in the configuration space of RSOS paths without the restriction (2.3). The paths are allowed to move in the lower half-plane and it is amusing to see what is the effect of changing the configuration space. If  $u = 1$ , one has a random walker with fixed ends at positions 0 and  $L$ . It is convenient to see the paths as describing an interface between tiles which fill part of a square and a rarefied gas of tiles. In Figure 21 we show such a path in the case  $L = 6$ . Out of a maximum of 9 tiles, the square is filled with 7 tiles.

To see how the model works, we take  $L = 4$ . There are 6 configurations in this case as shown in Figure 22.

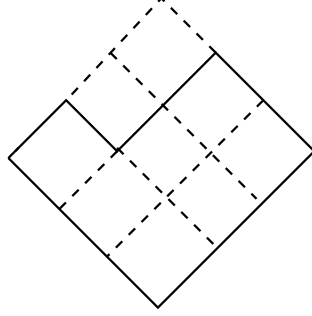


Figure 21: Configuration space for  $L = 6$ . The interface is a path which separates the seven tiles inside the square from a rarefied gas of tiles.

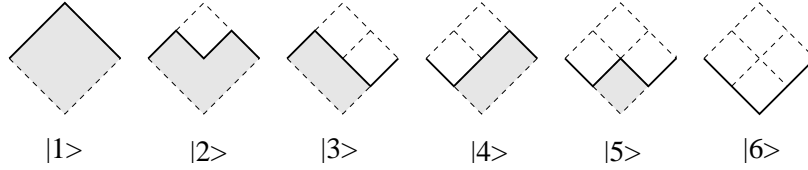


Figure 22: The six configurations for  $L = 4$ .

The Hamiltonian obtained using the rules of the flip-flop model is

$$H = - \begin{pmatrix} & |1\rangle & |2\rangle & |3\rangle & |4\rangle & |5\rangle & |6\rangle \\ \langle 1| & -1 & u & 0 & 0 & 0 & 0 \\ \langle 2| & 1 & -(2+u) & u & u & 0 & 0 \\ \langle 3| & 0 & 1 & -(1+u) & 0 & u & 0 \\ \langle 4| & 0 & 1 & 0 & -(1+u) & u & 0 \\ \langle 5| & 0 & 0 & 1 & 1 & -(2u+1) & u \\ \langle 6| & 0 & 0 & 0 & 0 & 1 & -u \end{pmatrix}. \quad (\text{A.1})$$

The wave function corresponding to the eigenvalue zero is:

$$u^4|1\rangle + u^3|2\rangle + u^2(|3\rangle + |4\rangle) + u|5\rangle + |6\rangle. \quad (\text{A.2})$$

In the stationary state, each configuration gets as a coefficient a monomial in  $u$  with an exponent equal to the number of tiles inside the square. The partition function is

$$Z_4(u) = 1 + u + 2u^2 + u^3 + u^4. \quad (\text{A.3})$$

One could have obtained directly (A.2) using the matrix-product method [20] for an open system with the processes given by (4.14) and (4.15). If a step up in the path is given by a generator  $U$  and a step down by a generator  $D$ , we can use the algebra

$$UD = uDU \quad (\text{A.4})$$

to find for example, that the coefficient of the configuration  $|1\rangle$  ( $UUDD$ ) gets a factor  $u^4$  compared with the configuration  $|6\rangle$  ( $DDUU$ ).

It is easy to show that the partition function  $Z_L(u)$  for  $L$  sites ( $L = 2n$ ) is

$$Z_{2n}(u) = \frac{(2n)_u!}{((n)_u!)^2} = \frac{(u^{n+1} - 1) \cdots (u^{2n} - 1)}{(u - 1)(u^2 - 1) \cdots (u^n - 1)}, \quad (\text{A.5})$$

where  $(n)_u! = 2_u 3_u \cdots n_u$  are  $u$ -factorials and

$$m_u = \frac{u^m - 1}{u - 1} \quad (\text{A.6})$$

It is easy to show that the number of tiles inside the square

$$N_L(u) = u \frac{d}{du} \ln Z_L(u) \quad (\text{A.7})$$

in the large  $L$  limit is:

$$\lim_L N_L(u) = \begin{cases} n^2 + C(u) & \text{if } u > 1 \\ n^2/2 & \text{if } u = 1 \\ -C(1/u) & \text{if } u < 1 \end{cases}, \quad (\text{A.8})$$

where  $C(u)$  is given by (4.13). This result is amusing since it shows that for any  $u > 1$ , in the large  $L$  limit, the important configurations are the same as for the flip-flop model. For  $u < 1$ , the relevant configurations are those near the empty square. They are obtained by a simple reflexion (top  $\rightarrow$  bottom) of the configurations relevant for  $u > 1$  (the Hamiltonian is invariant under the transformation  $u \rightarrow 1/u$  with a change of the time scale). At  $u = 1$ , one has the random walker.

The phase diagram of this model is the same as the one of the flip-flop model. The only difference between the two models in the large  $L$  limit is the heights profiles in the  $u < 1$  domain.

## References

- [1] Schmittmann B and Zia R K P, 1995 *Phase Transitions and Critical Phenomena* **17**, Eds Domb C and Lebowitz J (London: Academic)
- [2] Halpin-Healy T and Zhang Y-Ch, 1995 *Physics Reports* **254** 215
- [3] Edwards S F and Wilkinson D R, 1982 *Proc. Roy. Soc. London Series A* **381** 17
- [4] M. Kardar M, G. Parisi G, and Yi-C. Zhang Yi-C, 1986 *Phys. Rev. Lett.* **56** 889
- [5] Povolotsky A M and Priezhev V B, 2003 *J. Stat. Phys.* **111** 1149
- [6] Derrida B and Vannimenus J, 1983 *Phys. Rev. B* **27** 4401
- [7] de Gier J, Nienhuis B, Pearce P and Rittenberg V, 2003 *J. Stat. Phys.* **114**, 1, Alcaraz F C and Rittenberg V, 2007 *J. Stat. Mech.* **P07009**, Alcaraz F C , Pyatov P and Rittenberg V, 2008 . *J. Stat. Mech.* **P01006**

- [8] Razumov A V and Stroganov Yu G, 2004 *Theor. Math. Phys.* **138** 333, *Theor. Mat. Fiz.* **141** 1609
- [9] Razumov A V and Stroganov Yu G, 2005 *Theor. Math. Phys.* **142** 237
- [10] Cantini L and Sportiello A, 2011 *Journ. of Comb. Theory Series A* **118** 1549
- [11] Alcaraz F C and Rittenberg V, 2011 *J. Stat. Mech.* **P09030**
- [12] Rouse P E, 1953 *J. Chem. Phys.* **21** 1272; Orwoll R A and Stockmayer W H, 2007 *Advances in Chemical Physics: Stochastic Process in Chemical Physics* vol 15. ed K E Shuler (Hoboken:John Wiley & Sons); Iwata K and Kurata M, 1969 *J. Chem. Phys.* **50** 4008, Verdier P H, 1970 *J. Chem. Phys.* **52** 5512
- [13] Di Francesco P and Zinn-Justin P, 2005 *J. Phys. A* **38** L815
- [14] Alcaraz F C and Rittenberg V, 2010 *J. Stat. Mech.* **P03024**
- [15] Fuerlinger J and Hofbauer J, 1985 *J. of Combinatorial Theory* **A40** 248
- [16] Blythe R A, Evans M R, Colaiori F and Essler F H L, 2000 *J. Phys. A* **33** 2313
- [17] Read N and Saleur H, 2001 *Nucl. Phys. B* **613** 409
- [18] Family F and Vicsek E, 1985 *J. Phys. A* **18** L75
- [19] Derrida Bi, 2011 *private communication*
- [20] Blythe R A and Evans M R, 2007 *J. Phys. A: Math. Theor.* **40** R333
- [21] Kleis J and Schroeder E, 2005 *J. Chem. Phys.* **122** 164902
- [22] Knott M, Kaya H and Chan H S, 2004 *Polymer* **45** 63
- [23] Gay-Balmaz F, Holm D D, Putkaradaze V and Ratiu T S 2012 *Adv. Appl. Math.* **48** 535